Redistribution of elements in glass induced by a high-repetition-rate femtosecond laser

Fangfang Luo,[1,2] Bin Qian,[1,2] Geng Lin,[1,2] Jian Xu,[1,2] Yang Liao,[1,2] Juan Song,[3] Haiyi Sun,[1] Bin Zhu,[4] Jianrong Qiu,[4] Quanzhong Zhao,[1,*] and Zhizhan Xu[1]

[1]*State Key Laboratory of High Field Laser Physics, Shanghai Institute of Optics and Fine Mechanics, Chinese Academy of Sciences, Shanghai 201800, China*

[2]*Graduate School of the Chinese Academy of Sciences, Beijing 100039, China*

[3]*School of Materials Science and Engineering, Jiangsu University, Zhenjiang 212013, Jiangsu, China*

[4]*State Key Laboratory of Silicon Materials, Zhejiang University, Hangzhou 310027, China*

** zqz@siom.ac.cn*

Abstract: The redistribution of elements in a multicomponent oxyfluoride glass is induced by a 250 kHz femtosecond laser. Elemental distribution in the cross section of the modified region along the laser propagation axis is analyzed by an electron microprobe analyzer. The results indicate that the relative concentrations of network formers of the glass are higher in the central area of the modified region and lower in the periphery of the modified region compared with the unirradiated areas. However, the relative concentrations of network modifiers are as opposed to that of network formers. Fluorescence spectra confirm that the distribution of fluorescence intensity of Yb^{3+} in the modified region is consistent with that of its concentration. The effects of spherical aberration of the incident beam on the elemental redistribution are also discussed.

OCIS codes: (160.2750) Glass and other amorphous materials; (350.3390) Laser materials processing

References and links

1. R. R. Gattass, and E. Mazur, "Femtosecond laser micromachining in transparent materials," Nat. Photonics **2**(4), 219–225 (2008).
2. M. Ams, G. D. Marshall, P. Dekker, M. Dubov, V. K. Mezentsev, I. Bennion, and M. J. Withford, "Investigation of ultrafast laser–photonic material interactions: challenges for directly written glass photonics," IEEE J. Sel. Quant. Electron. **14**(5), 1370–1381 (2008).
3. C. T. Hebeisen, G. Sciaini, M. Harb, R. Ernstorfer, S. G. Kruglik, and R. J. D. Miller, "Direct visualization of charge distributions during femtosecond laser ablation of a Si (100) surface," Phys. Rev. B **78**(8), 081403 (2008).
4. S. Kanehira, J. Si, J. Qiu, K. Fujita, and K. Hirao, "Periodic nanovoid structures via femtosecond laser irradiation," Nano Lett. **5**(8), 1591–1595 (2005).
5. K. M. Davis, K. Miura, N. Sugimoto, and K. Hirao, "Writing waveguides in glass with a femtosecond laser," Opt. Lett. **21**(21), 1729–1731 (1996).
6. C. B. Schaffer, A. Brodeur, J. F. García, and E. Mazur, "Micromachining bulk glass by use of femtosecond laser pulses with nanojoule energy," Opt. Lett. **26**(2), 93–95 (2001).
7. A. M. Streltsov, and N. F. Borrelli, "Fabrication and analysis of a directional coupler written in glass by nanojoule femtosecond laser pulses," Opt. Lett. **26**(1), 42–43 (2001).
8. T. Kondo, S. Matsuo, S. Juodkazis, and H. Misawa, "Femtosecond laser interference technique with diffractive beam splitter for fabrication of three-dimensional photonic crystals," Appl. Phys. Lett. **79**(6), 725 (2001).
9. S. M. Eaton, H. Zhang, M. L. Ng, J. Li, W. J. Chen, S. Ho, and P. R. Herman, "Transition from thermal diffusion to heat accumulation in high repetition rate femtosecond laser writing of buried optical waveguides," Opt. Express **16**(13), 9443–9458 (2008).
10. S. M. Eaton, H. Zhang, P. R. Herman, F. Yoshino, L. Shah, J. Bovatsek, and A. Y. Arai, "Heat accumulation effects in femtosecond laser-written waveguides with variable repetition rate," Opt. Express **13**(12), 4708–4716 (2005).
11. W. J. Yang, C. Corbari, P. G. Kazansky, K. Sakaguchi, and I. C. Carvalho, "Low loss photonic components in high index bismuth borate glass by femtosecond laser direct writing," Opt. Express **16**(20), 16215–16226 (2008).

#121856 - $15.00 USD Received 21 Dec 2009; revised 4 Feb 2010; accepted 16 Feb 2010; published 12 Mar 2010

12. K. Miura, J. Qiu, S. Fujiwara, S. Sakaguchi, and K. Hirao, "Three-dimensional optical memory with rewriteable and ultrahigh density using the valence-state change of samarium ions," Appl. Phys. Lett. **80**(13), 2263–2265 (2002).
13. Y. Dai, B. Zhu, J. Qiu, H. Ma, B. Lu, S. Cao, and B. Yu, "Direct writing three- dimensional Ba2TiSi2O8 crystalline pattern in glass with ultrashort pulse laser," Appl. Phys. Lett. **90**(18), 181109 (2007).
14. Y. Liu, B. Zhu, L. Wang, Y. Dai, H. Ma, and J. Qiu, "Femtosecond laser induced coordination transformation and migration of ions in sodium borate glasses," Appl. Phys. Lett. **92**, 121113/1–3 (2008).
15. S. Kanehira, K. Miura, and K. Hirao, "Ion exchange in glass using femtosecond laser irradiation," Appl. Phys. Lett. **93**(2), 023112 (2008).
16. Y. Liu, M. Shimizu, B. Zhu, Y. Dai, B. Qian, J. Qiu, Y. Shimotsuma, K. Miura, and K. Hirao, "Micromodification of element distribution in glass using femtosecond laser irradiation," Opt. Lett. **34**(2), 136–138 (2009).
17. K. Miura, K. Hirao, Y. Shimotsuma, M. Sakakura, and S. Kanehira, "Formation of Si structure in glass with a femtosecond laser," Appl. Phys., A Mater. Sci. Process. **93**(1), 183–188 (2008).
18. A. Marcinkevičius, V. Mizeikis, S. Juodkazis, S. Matsuo, and H. Misawa, "Effect of refractive index-mismatch on laser microfabrication in silica glass," Appl. Phys. A Mater. Sci. Process. **76**(2), 257–260 (2003).
19. C. Hnatovsky, R. S. Taylor, E. Simova, V. R. Bhardwaj, D. M. Rayner, and P. B. Corkum, "High-resolution study of photoinduced modification in fused silica produced by a tightly focused femtosecond laser beam in the presence of aberration," J. Appl. Phys. **98**(1), 013517 (2005).
20. N. Huot, R. Stoian, A. Mermillod-Blondin, C. Mauclair, and E. Audouard, "Analysis of the effects of spherical aberration on ultrafast laser-induced refractive index variation in glass," Opt. Express **15**(19), 12395–12408 (2007).
21. C. Mauclair, A. Mermillod-Blondin, N. Huot, E. Audouard, and R. Stoian, "Ultrafast laser writing of homogeneous longitudinal waveguides in glasses using dynamic wavefront correction," Opt. Express **16**(8), 5481–5492 (2008).
22. J. Song, X. Wang, X. Hu, Y. Dai, J. Qiu, Y. Cheng, and Z. Xu, "Formation mechanism of self-organized voids in dielectrics induced by tightly focused femtosecond laser pulses," Appl. Phys. Lett. **92**(9), 092904 (2008).
23. S. Ye, B. Zhu, J. Chen, J. Luo, and J. Qiu, "Infrared quantum cutting in Tb^{3+},Yb^{3+} codoped transparent glass ceramics containing CaF_2 nanocrystals," Appl. Phys. Lett. **92**(14), 141112 (2008).
24. Y. Liu, M. Shimizu, X. Wang, B. Zhu, M. Sakakura, Y. Shimotsuma, J. Qiu, K. Miura, and K. Hirao, "Confocal Raman imaging of femtosecond laser induced microstructures in germanate glasses," Chem. Phys. Lett. **477**(1-3), 122–125 (2009).
25. C. B. Schaffer, J. F. Garcia, and E. Mazur, "Bulk heating of transparent materials using a high-repetition-rate femtosecond laser," Appl. Phys., A Mater. Sci. Process. **76**(3), 351–354 (2003).
26. K. Hirao, and K. Miura, ""Writing waveguides and gratings in silica and related materials by a femtosecond laser," J. Non-Crys," Sol. **239**, 91–95 (1998).
27. L. Sudrie, A. Couairon, M. Franco, B. Lamouroux, B. Prade, S. Tzortzakis, and A. Mysyrowicz, "Femtosecond laser-induced damage and filamentary propagation in fused silica," Phys. Rev. Lett. **89**, 186601/1–4 (2002).
28. P. Török, P. Varga, and G. Nèmeth, "Analytical solution of the diffraction integrals and interpretation of wave-front distortion when light is focused through a planar interface between materials of mismatched refractive indices," J. Opt. Soc. Am. A **12**(12), 2660–2671 (1995).

1.Introduction

Femtosecond laser micromachining of transparent materials has unique advantages over the continuous wave and long-pulse laser micromachining because of the nonlinear nature of the absorption independent of the material [1]. When a single intense ultrashort laser pulse is tightly focused inside glass samples, it will induce nonlinear processes including multiphoton ionization, tunneling ionization or avalanche ionization [2], and result in complicated dynamics (melting, evaporation, phase explosion, thermal plasma generation etc.) [3]. Therefore, various three dimensional microstructures inside transparent materials have been fabricated by femtosecond lasers, such as periodic nanosized voids [4], waveguides [5,6], couplers [7], photonic crystals [8] and so on.

Recently, high-repetition-rate femtosecond (HRRFS) lasers have attracted considerable attentions for their heat accumulation effect as well as the relatively low energy of single laser pulse. These properties of HRRFS lasers make it possible to form low-loss optical waveguides with higher writing speed [9–11] and fabricate nonlinear optical devices inside glasses [12,13]. At the same time, a novel laser-matter interaction induced by HRRFS laser is reported [14–17]. When an intense HRRFS laser is tightly focused inside a glass sample, the distribution of elements is proved to be modified in a range of a few tens of micrometers around the focal point, perpendicular to the laser propagation axis. Accordingly, the refractive

#121856 - $15.00 USD Received 21 Dec 2009; revised 4 Feb 2010; accepted 16 Feb 2010; published 12 Mar 2010

index around the focal point is modified. This result is helpful for the fabrication of photonic devices or waveguides. However, we found that all the work is focused on the redistribution of elements in the cross section perpendicular to the laser propagation axis. The information of elemental distribution in the cross section along the laser propagation axis lacks and needs investigation. As a matter of fact, when a laser with low- or high-repetition-rate is focused inside a transparent material, the spherical aberration (SA) due to an index mismatch between air and material exists, which has an effect on the longitudinal stretch (parallel to the laser propagation axis) of the focal volume along with a modulation in the longitudinal intensity profile [18–22]. So, it is essential to investigate element redistribution affected by SA when glasses are irradiated by HRRFS lasers.

In this article, we investigate the distribution of elements in the cross section of focal region along the laser propagation axis for a multicomponent oxyfluoride glass irradiated by a 250 kHz femtosecond laser. We found that the relative concentrations of network formers Si^{4+}, O^{2-} and Al^{3+} ions of the glass sample are higher in the central area of the focal region and lower in the periphery of the focal region compared with the unirradiated areas. However, the relative concentrations of network modifiers Ca^{2+}, Yb^{3+} and F^{-} ions are as opposed to that of network formers. The effects of SA on the elemental redistribution are also discussed.

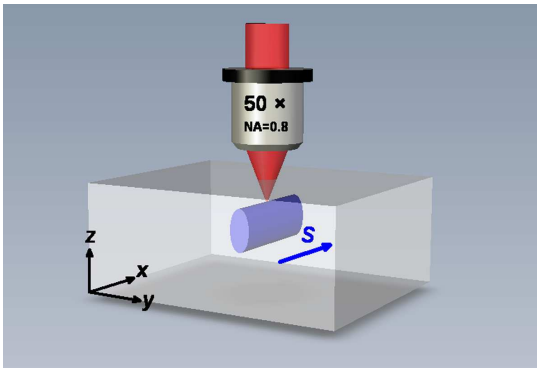

Fig. 1. Schematic of the laser writing.

2. Experimental

A glass sample with composition of $60SiO_2$-$20Al_2O_3$-$20CaF_2$-$10YbF_3$ (mol %) is used in this study, which is prepared by the conventional melt-quenching method. Detailed fabrication of the glass was described elsewhere [23]. The sample is cut and polished into blocks 10 × 3 × 2 mm^3 in size. Then it is mounted on a xyz stage with a resolution of 1 μm, which is precisely controlled by a computer for laser micromachining. The schematic of the micromachining process is shown in Fig. 1. A regeneratively amplified 800 nm Ti: sapphire laser emitting a train of 150 fs, 250 kHz mode-locked pulses is used for laser direct writing. The direction of polarization of the laser is parallel to the x-axis. The laser pulse with energy of 2 μJ is focused via a microscope objective (50 × , NA = 0.8) into the sample. The transmission ratio of the used objective is around 70%, by considering its truncation ratio of ~15%, the pulse energy is 1.19 μJ after the objective. The laser focus is located at about 50 μm beneath the surface of the sample. Consider the refractive index of the glass sample (n is around 1.5), the real depth should be 75 μm. The sample is translated at a speed of 10 μm/s along the x-axis, perpendicular to the laser propagation axis (z axis). After laser irradiation, the sample is side polished until the surface is at the level of the internal modified structures, which are imaged under an optical microscope in transmission mode. An electron microprobe analyzer (EPMA: JEOL, JXA-8100) is used to determine the relative concentrations of the elemental composition in these structures. A Raman spectrometer (Renishaw inVia) with a 785 nm laser excitation is employed to measure the confocal fluorescence spectra.

#121856 - $15.00 USD Received 21 Dec 2009; revised 4 Feb 2010; accepted 16 Feb 2010; published 12 Mar 2010

3. Results and discussion

Figure 2(a) shows the optical microscope image of the cross section of the laser-modified zone along y-z plane. There is a bright gray zone in the periphery of the photo-modified area, which is attributed to strains resulted from thermal expansion [24]. Within the periphery, we can see that the whole modified area is black. The variable acts of melting and solidifying across the innear region result in local densification, the formation of color centers and defect generation [9,10,25,26]. The results lead to the non-uniformity of the light absorption and the refractive index, which is the possible reason for color contrast in the optical image. By inserting the sample to the middle of two cross polarizers, we also check whether birefringent effect occurs in the laser modified area. We found that the birefringent effect cannot be observed in the black area but can be observed in the surrounding areas. In the following sections, only the black area is discussed as the modified area. The maximum longitudinal and transversal lengths of this zone are 44.1 and 29.6 μm, respectively. There are two possible effects for the longitudinal stretch being longer than the laser focal volume. One is the self-focusing effect, the other one is the SA effect. Sudrie *et al*. reported that it can be attributed to a filamentary propagation [27]. However, the aspect ratio in their results is ~6.8, which is bigger than that in ours, ~1.5, and no narrow track appears in ours. It means that the self-focusing of the laser beam induced by the optical Kerr effect is not the main reason to produce our results. Additionally, a high numerical aperture microscope objective we used is in favor of reducing the optical Kerr effect and enhancing SA. The influence of SA on the longitudinal extent will be discussed in the latter part.

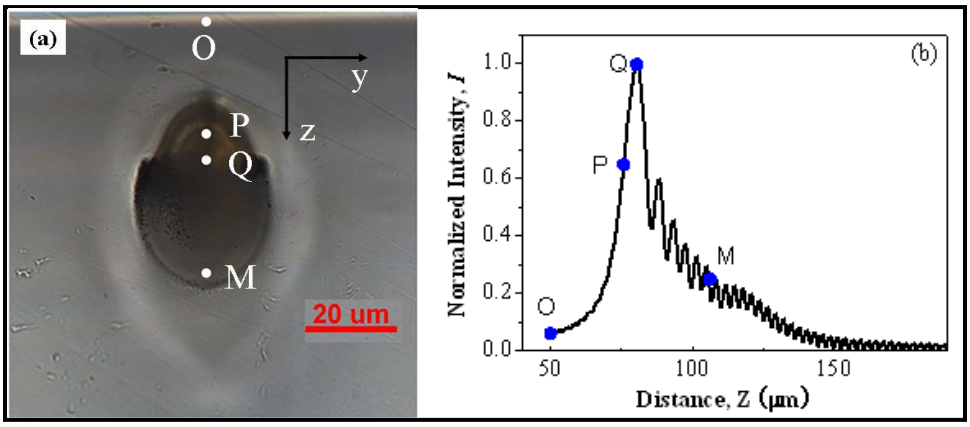

Fig. 2. (a) Optical microscope image of yz-plane of the modified structure in glass. (b) The normalized on-axis fluence distribution with consideration of the spherical aberration effect at the focal depth of 50 μm through an objective with NA = 0.8. This simulation is based on the model of Ref [28].

By employing the geometrical considerations in Refs. 18-22 and our experimental parameters, we can quantificationally determine the longitudinal spherical aberration l = PM = 30.7 μm, where the position of point P is 25 μm away from the focal point O (Point O is the focus point in the absence of the refractive index mismatch, point P is the paraxial focus and point M is the marginal focus, given by Refs [18–22].). The points O, P and M are labeled in Fig. 2. Apparently, the longitudinal length of the modified structure in Fig. 2 is longer than PM, and the transverse width is larger than the size of beam waist diameter, estimated to be ~1.2 μm. The discrepancy can be explained by the heat accumulation effect [10,25]. By using the way of static exposure of high-repetition-rate laser, Schaffer *et al.* [24] and Eaton *et al*. [10] present photo-modified zone larger than the focal volume in glass, and simulate the cumulative heating to explain it. So, we can conclude that the heat accumulation effect is the

#121856 - $15.00 USD Received 21 Dec 2009; revised 4 Feb 2010; accepted 16 Feb 2010; published 12 Mar 2010

main reason for longitudinal axial length of the modified area large than PM as well as radical expansion.

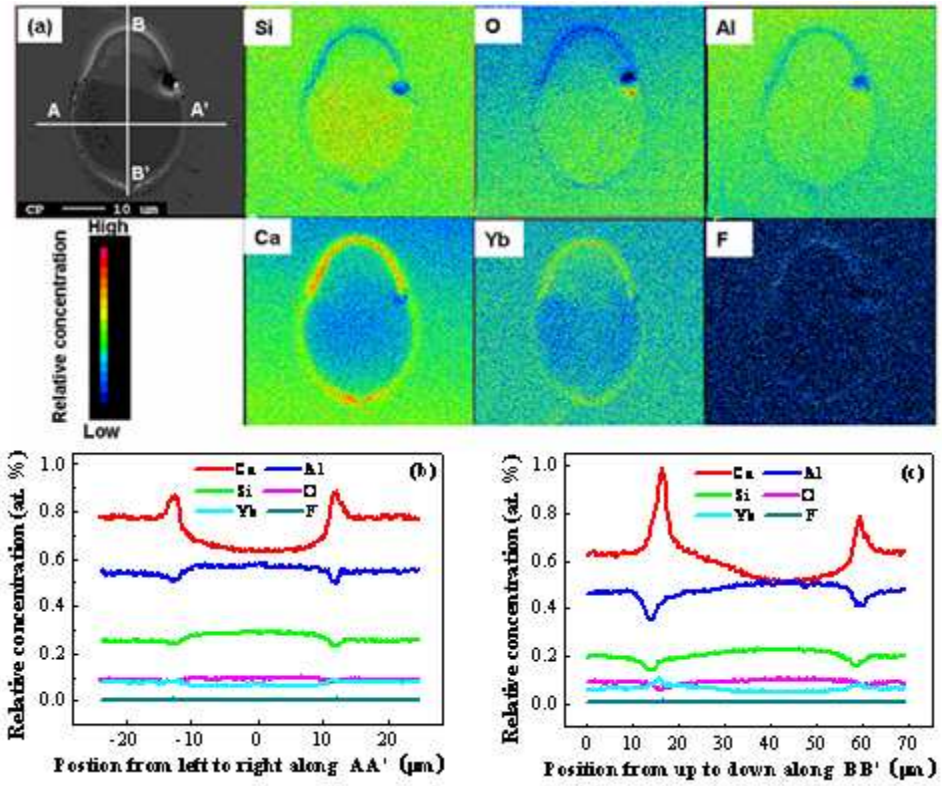

Fig. 3. (a) Mapping of elemental distribution of the modified area in yz-plane measured by EPMA. (b) and (c) Relative concentration profiles of each ion along line AA´ and line BB´ in the backscattering image, respectively.

Figure 3(a) shows the backscattering electron image and the profiles of the relative concentrations of different elements of the modified area in glass on the polished y-z plane, analyzed by the EPMA. It is obvious that the profiles of the relative concentrations of different elements correspond to the modified zone in the microscopic image (Fig. 2). One can see that the relative concentrations of network formers Si^{4+}, O^{2-}, and Al^{3+} ions of the glass are higher in the central area of the modified structure and lower in the periphery of the modified structure compared with the unirradiated areas. However, the concentration distribution of network modifiers Ca^{2+}, Yb^{3+} and F^{-} ions is opposite to that of network formers. Figures 3(b) and 3(c) show the results of line-scan analysis of the relative atomic concentration along line AA´ and line BB´ drawn in the backscattering electron image. The changing tendency of the relative concentrations of all ions is symmetric along line AA´. However, it is asymmetric along line BB´. For example, the maximum concentration of the modifier Ca^{2+} ions on the top is higher than that on the bottom. The distance from the maximum concentration on the top to the minimum concentration in the central area is 27.5 μm, while it is 16.6 μm from the maximum concentration on the bottom to the minimum concentration in the central area. Therefore, the distribution of all ions' concentration possesses axis symmetry in y-z plane. These results indicate that redistribution of elements is realized in the modified region.

We further investigate the confocal fluorescence spectra of the modified area as shown in Fig. 4. Figure 4(a) shows the confocal fluorescence spectra from the marked positions of the modified area. When the excitation wavelength is 785 nm, we can find an emission peak at

#121856 - $15.00 USD Received 21 Dec 2009; revised 4 Feb 2010; accepted 16 Feb 2010; published 12 Mar 2010

975 nm which can be attributed to the transition $^2F_{5/2}$ - $^2F_{7/2}$ of Yb^{3+} ions. The intensity of point A at the top edge is higher than points B and C in the central zone which coincides with distribution of concentration of Yb^{3+} ions. Figures 4(b) and 4(c) present the distribution of the fluorescence intensity at 975 nm along the transversal and longitudinal scanning lines in the insets. We can clearly see that the changing tendency of the fluorescence intensity in Figs. 4(b) and 4(c) is consistent with that of relative concentrations of Yb^{3+} ions in Figs. 3(b) and 3(c). Therefore, we can conclude that the relative concentration change, i.e., redistribution of elements, is the main reason for the fluorescence intensity change.

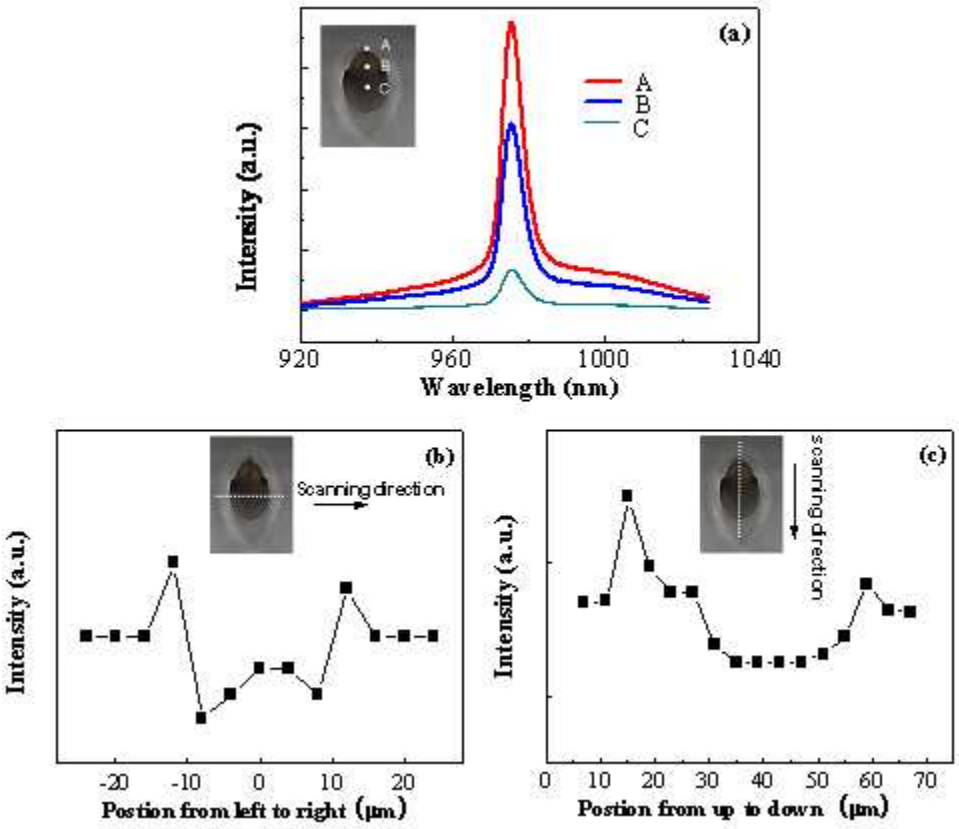

Fig. 4. (a) Fluorescence spectra of the marked areas in the modified structure (excitation wavelength 785 nm). (b) and (c) Fluorescence intensity at 975 nm along the transversal and longitudinal scanning lines in the insets, respectively.

The migrating tendency of the network formers and the network modifiers in our results agrees with those of previous observations [15,16]. The network formers gather in the central area of the modified structure, while the network modifiers assemble at the margin. We think that it is attributed to the different diffusion coefficients between the network formers and the modifiers [16]. When HRRFS laser pulses are focused inside a glass sample, the exposed region transforms into a liquid state followed by some bonds among ions broken. Meanwhile, the laser-induced temperature difference will result in the pressure difference from the central area to the margin, driving ions away from the focal point. Under the above-mentioned conditions, glass network modifiers will diffuse more intensively away from the central area of the modified structure than network formers, because of higher diffusion coefficient. As a result, the relative concentrations of network modifiers of the glass are relatively higher at the

#121856 - $15.00 USD Received 21 Dec 2009; revised 4 Feb 2010; accepted 16 Feb 2010; published 12 Mar 2010

margin of the modified zone and lower in the central area. The distribution of the relative concentrations of network formers is opposite to that of network formers.

To demonstrate the influence of the SA on the longitudinal extent of the laser affected zone, the laser beam with the pulse energies of 1.19 and 1.38 μJ (after objective) is focused inside the glass sample at five different focusing depths (120, 195, 270, 345, and 450 μm) by the same irradiation conditions. The affected zones along y-z plane are presented in Fig. 5. As can be seen, although the affected zone has similar distorted shape, the longitudinal and transversal sizes of the affected zone decreased with the increasing of focusing depth at fixed incident energy. Our results coincide with that reported in Ref. 18. Although the level of the refractive index mismatch in Ref. 18 is less than that in our case, the changing tendency of the axial intensity induced by SA is similar. The decreased size of the affected zones with the focusing depth in our result is due to the decreased axial intensity. Therefore, we can conclude that the SA effect is the main point of the stretch of the laser-modified zone.

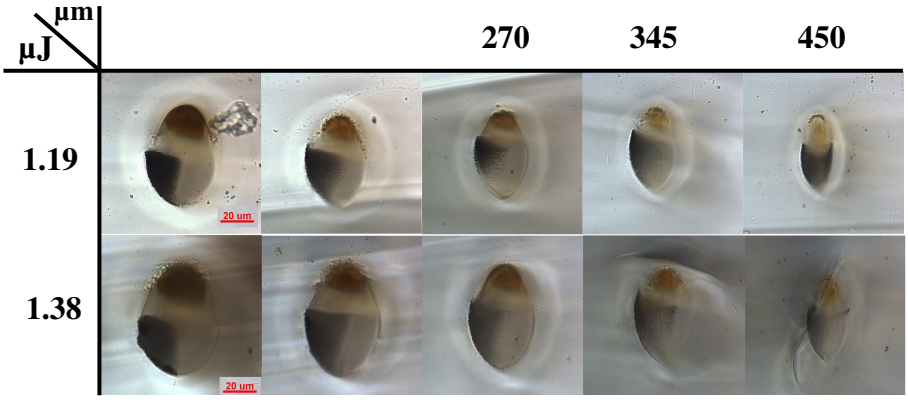

Fig. 5. Effect of focusing depth beneath the glass surface on the laser modified area with the presence of spherical aberration.

In order to clarify the effect of SA on the distribution of elements, we simulate the on-axis laser fluence distribution by adopting the theory of P. Török *et al*. [28], as shown in Fig. 2 (b). Considering the beam truncation value in our case, we used a near uniform illumination, which will favor the appropriateness of their simulation [28]. The fluence distribution from the focal point O to the paraxial focal point P experiences a weak growth in a long distance and then a sharp increase around point P up to the maximum value at point Q (PQ = 5.7 μm). A quasi-periodic oscillation between maximum and minimum accompanied by a dramatic drop in the maximum value also can be observed. According to the heat accumulation effect, higher laser fluence will result in a zone of higher temperature [10,24]. As a result, when a laser is focused into a glass sample, there is a large temperature difference between the top edge of the modified structure and point Q, as well as the bottom edge and point Q. Apparently, the increasing tendency of temperature based on the intensity z-distribution between the top edge and point Q is faster than the decreasing tendency of temperature between point Q and the bottom edge. So the pressure difference of the former is bigger than that of the latter. The larger the pressure difference is, the stronger the driving force of the ion diffusivity is. Therefore, the maximum value of the element distribution of the network modifiers and minimum value of the element distribution of the network formers are at the top edges of the modified structures [Fig. 3(c)]. Meanwhile, the second extremum is at the bottom edges of the structures [Fig. 3(c)]. It is noteworthy that the minimum value of network formers appears at the zone 12.3 μm away from point Q instead of that near point Q, which is

#121856 - $15.00 USD Received 21 Dec 2009; revised 4 Feb 2010; accepted 16 Feb 2010; published 12 Mar 2010

against the influence of the temperature gradient. This difference indicates some other effects should be considered.

4. Conclusion

The redistribution of elements is realized by using a 250 kHz femtosecond laser irradiation of a multicomponent oxyfluoride glass. Experimental results determined by EPMA indicate that the relative concentrations of all ions in the glass sample are cylindrically symmetric along the laser propagation direction, and the relative concentrations of network formers are higher in the central area of the modified regions and lower in the periphery of the modified regions compared with the unirradiated areas. However, the concentration distribution of network modifiers is opposite to that of network formers. The fluorescence intensity change of Yb^{3+} ions in the modified structure confirms the relative concentration change. We consider that SA effect and the heat accumulation effect are responsible for the redistribution of elements. Our results are helpful for the fabrication of three dimensional waveguide-type photonic devices inside glasses.

Acknowledgments

The authors gratefully acknowledge Dr. Z. H. Zhou and Mr. X. M. He of Shanghai Institute of Optics and Fine Mechanics for their experimental help.This work was financially supported by National Natural Science Foundation of China (Grant Nos. 50672087 and 60778039), National Basic Research Program of China (2006CB806007), and Changjiang Scholars and Innovative Research Team in University (IRT0651).

#121856 - $15.00 USD Received 21 Dec 2009; revised 4 Feb 2010; accepted 16 Feb 2010; published 12 Mar 2010